An Experimental and Density Functional Theoretical Investigation of Iron-57 Mössbauer Quadrupole Splittings in Organometallic and Heme-Model Compounds: Applications to Carbonmonoxy-Heme Protein Structure†

Robert H. Havlin,[¶,§] Nathalie Godbout,[§] Renzo Salzmann,[‡,§] Mark Wojdelski,[||,§] William Arnold,[#,§] Charles E. Schulz,[⊥] and Eric Oldfield*[,§]

Contribution from the Department of Chemistry, University of Illinois at Urbana−Champaign, 600 South Mathews Avenue, Urbana, Illinois 61801, and Department of Physics, Knox College, 2 East South Street, Galesburg, Illinois 61401

Received July 31, 1997. Revised Manuscript Received December 4, 1997

Abstract: We have investigated the ^{57}Fe Mössbauer quadrupole splittings in the following compounds by using density functional theory, and in some cases via experiment: $Fe(CO)_3$(*cyclo*-butadiene), $Fe(CO)_5$, $Fe(CO)_3$(1,4−butadiene), $CpFe(CO)_2Me$, $Fe(CO)_3$(propenal), $CpFe(CO)_2Cl$, (CO)(pyridine)$(DMGBPh_2)_2$Fe(II) (DMG = dimethylglyoximato), (CO)(pyridine)$(DMGBBN)_2$Fe(II) (BBN = 9-borabicyclo[3.3.1]nonane), (CO)(1-methylimidazole)(5,10,15,20-tetraphenylporphinato)Fe(II), (CO)(pyridine)(5,10,15,20-tetraphenyl-porphinato)Fe(II), (nitrosobenzene)(pyridine)(5,10,15,20-tetraphenylporphinato)Fe(II), $(pyridine)_2$(5,10,15,20-tetraphenylporphinato)Fe(II), $(1\text{-methylimidazole})_2$(5,10,15,20-tetramesitylporphinato)Fe(II), and $(trimethylphosphine)_2$(2,3,7,8,12,13,17,18-octaethylporphinato)Fe(II). The electric field gradients at iron were evaluated by using a locally dense basis approach: a Wachters' all electron representation for iron, a 6-311++G^{2d} basis for all atoms directly bonded to iron, and either a 6-31G* basis for all other atoms or, in the case of the metalloporphyrins, a 6-31G*/3-21G* or 4-31G* basis, with the smaller basis being used on the peripheral atoms. Using a value of 0.16×10^{-28} m^2 for the quadrupole moment of ^{57}Fe^m, we find good agreement between theoretical and experimental quadrupole splittings: a slope of 1.04, an R^2 value of 0.975, and a root-mean-square error of 0.18 mm s^{-1}, for the 14 compounds examined. We have also investigated the effects of the CO ligand tilt and bend on the ^{57}Fe quadrupole splittings in several heme models. The theoretical results provide no support for the very large (40°) Fe−C−O bond angles suggested by several diffraction studies on *Physeter catodon* carbonmonoxymyoglobin ($P2_1$ crystals). In contrast, the experimental results for (CO)(1-MeIm)(5,10,15,20-tetraphenylporphinato)Fe(II), which contains a linear and untilted Fe−CO, are in very close accord with the experimental values for CO-myoglobin: 0.35 mm s^{-1} for the model system versus 0.363−0.373 mm s^{-1} for MbCO, with V_{zz} oriented perpendicular to the porphyrin plane, as found experimentally. Calculations on metalloporphyrins at the more distorted X-ray geometries yield quadrupole splittings around 2 mm s^{-1}, inconsistent with experiment.

Introduction

The nature of metal−ligand bonding in heme proteins has been the topic of lively debate for over 30 years.[1−5] In principle, one of the more powerful spectroscopic techniques for probing the iron center is ^{57}Fe Mössbauer spectroscopy.[6,7] However, there has been relatively little work reported on the theoretical analysis of iron-57 Mössbauer data in organometallic, metalloporphyrin, and protein systems.[8−10] The principal reasons for this are that, first, heme protein structures are themselves part of the focus of the debate,[5] and without a good initial structure the problem of computing spectroscopic observables becomes more difficult. Second, the level of theory needed to compute Mössbauer quadrupole splittings has been uncertain.[10] Electron

† This work was supported by the United States Public Health Service (National Heart, Lung and Blood Institute, Grant No. HL-19481).

§ University of Illinois at Urbana−Champaign.

⊥ Knox College.

¶ Barry Goldwater Fellow. Present Address: Department of Chemistry, University of California at Berkeley, Berkeley, CA 94720.

‡ Swiss National Science Foundation Postdoctoral Research Fellow, 1996−1997; American Heart Association, Inc., Illinois Affiliate, Postdoctoral Research Fellow, 1997−1998.

|| Colgate-Palmolive Scholar.

GAANN Fellow.

(1) Pauling, L. *Nature* **1964**, *203*, 182−183.

(2) Weiss, J. J. *Nature* **1964**, *203*, 183.

(3) Park, K. D.; Guo, K.; Adebodun, F.; Chiu M. L.; Sligar, S. G.; Oldfield, E. *Biochemistry* **1991**, *30*, 2333−2347.

(4) Ray, G. B.; Li, Z.-Y.; Ibers, J. A.; Sessler, J. L.; Spiro, T. G. *J. Am. Chem. Soc.* **1994**, *116*, 162−176.

(5) Lim, M.; Jackson, T. A.; Anfinrud, P. A. *Science* **1995**, *269*, 962−966.

(6) Sams; J. R.; Tsin, T. B. *The Porphyrins* **1979**, *4*, 425−478.

(7) Debrunner, P. G. *Iron Porphyrins* Lever, A. B. P., Gray, H. B., Eds.; VCH Publishers: New York, 1989; Vol. 3, pp 139−234.

(8) Trautwein, A. In *Structure and Bonding*; Dunitz, J. D., Hemmerich, P., Holm, R. H., Ibers, J. A., Jørgensen, C. K., Neilands, J. B., Reinen, D., Williams, R. J. P., Eds.; Springer-Verlag: New York, 1974; Vol. 20, pp 101−166.

(9) Buhl, M. L.; Long, G. J. *J. Organomet. Chem.* **1993**, *461*, 177−185. Buhl, M. L.; Long, G. J.; Doyle, G. *J. Organomet. Chem.* **1993**, *461*, 187−199.

(10) Case, D. A.; Huynh, B. H.; Karplus, M. *J. Am. Chem. Soc.* **1979**, *101*, 4433−4453. Karpov, A. A.; Khleskov, V. I.; Smirnov, A. B. *Z. Strukt. Khim.* **1993**, *34*, 90−93.

S0002-7863(97)02619-X CCC: $15.00
Published on Web 03/13/1998

correlation effects might possibly play a role, but until recently efficient methods for the incorporation of electron correlation (and exchange) have been computationally expensive. Third, the relatively large size of porphyrin macrocycles exacerbates the cost of high level theoretical calculations greatly, so that highly simplified models such as $(NH_2)_4$ and bis(amidinato) fragments have frequently been used,[11,12] and few direct comparisons with experiment have been possible. Fourth, Sternheimer corrections, which are not always known to high accuracy, have been used in some calculations. As a result, unambiguous correlations between theory and experiment for metalloporphyrins and metalloproteins have not been forthcoming. Fortunately, however, there have been many recent developments in the use of density functional theory (see e.g. ref 13), which has the computational advantage that formal speed typically scales as N^3 (where N is the number of basis functions), rather than the $\gtrsim N^5$ for other correlated methods, resulting in a number of accurate electric field gradient tensor calculations, e.g. for ^{2}H,$^{35/37}$Cl, and ^{127}I.[14,15] These developments, when coupled with recent hardware improvements, encouraged us to reinvestigate ^{57}Fe Mössbauer quadrupole splittings (which are related to the computationally determined ^{57}Fe electric field gradients, EFGs) in a series of small organometallic model compounds, as well as in several macrocycles: bis(dimethylglyoximato)Fe(II) complexes, and in porphyrin macrocycles as well. Using parallel processing, we find that ^{57}Fe EFGs can now be readily evaluated, even in metalloporphyrins, at least for low-spin d^6 complexes. In this paper, we discuss primarily results on CO-hemes, but the general approach is equally applicable to O_2, RNC, RNO, and R_2S ligand binding in other systems as well, and has the advantage over other methods that not only are Sternheimer corrections not necessary,[16] but as a bonus, ^{57}Fe NMR chemical shifts are available from the calculations as well.[17,18]

Experimental Section

Synthetic Aspects. The following compounds were synthesized by using standard methods: $Fe(CO)_3$(*cyclo*-butadiene),[19] $CpFe(CO)_2Me$,[20] $Fe(CO)_3$(propenal),[21] $CpFe(CO)_2Cl$,[22] (CO)(pyr)(DMGBPh$_2$)$_2$Fe(II) (DMG = dimethylglyoximato),[23] (CO)(pyr)(DMGBBN)$_2$Fe(II) (BBN = 9-borabicyclo[3.3.1]nonane),[23] and (CO)(pyr)(5,10,15,20-tetraphenylporphinato)Fe(II).[24] (CO)(1-methylimidazole)(TPP)Fe(II) and (PhNO)(pyr)(TPP)Fe(II) (TPP = 5,10,15,20-tetraphenylporphinato) were both prepared from (TPP)FeCl, and their structures determined crystallographically. The synthesis and structure of (PhNO)(pyr)(TPP)Fe(II) and the *N*-methylimidazole adduct of TPP, (CO)(1-MeIm)(TPP)Fe(II), will be discussed elsewhere.[25,26]

$Fe(CO)_5$ was purchased from Aldrich (Milwaukee, WI) and $Fe(CO)_3$(1,4-butadiene) from Alfa (Ward Hill, MA).

Mössbauer Spectroscopy. For ^{57}Fe Mössbauer spectroscopic measurements, we used a Ranger Scientific, Inc. (Burleson, TX) MS-900 Mössbauer spectrometer equipped with a VT-900 transducer and a Kr-CO_2 gas proportional counter. The source was ^{57}Co in a 6 μm rhodium foil having an 8 mm active diameter, and an initial activity of 25 mCi (Amersham Life Sciences, Arlington, Heights, IL). Zero-field measurements were performed at low temperatures by using a Janis Model 10DT SuperVaritemp cryostat (Janis Research Company, Inc., Wilmington, MA). High-field measurements utilized a Janis Model 9TMOSS-0M-1.5 cryostat, which consists of a 9 T peak-field superconducting magnet having its field parallel to the γ-ray beam, together with a bucking coil to provide zero-field at the source position. The transducer for the high-field measurements was a "home-built" version of the Ranger VT-900 adapted for vertical operation with a vacuum enclosure. Samples were sealed in thin delrin containers using epoxy resin.

Computational Aspects. All electric field gradient calculations were performed by using the Gaussian-94[27] program. Small molecule calculations were carried out on International Business Machines (Austin, TX) RS/6000 computers (Models 340, 350, 360, 365, and 3CT), while the larger systems were investigated by using Silicon Graphics/Cray Research (Mountain View, CA) Origin-200, Origin-2000, and Power Challenge multiple processor machines, in parallel. For the small molecules, we used both X-ray and quantum chemical geometry optimized structures. These geometry optimizations were based on the methods used by Bühl for ^{57}Fe chemical shift calculations,[28] and basically involved using Wachters' all electron basis for iron,[29,30] Pople's[31] 6-31G* basis for all other atoms, and a Becke-Perdew (BP86) exchange-correlation functional.[32] For these model compounds, the EFGs were then calculated by using Becke's three parameter functional[33] with the Lee, Parr, and Yang correlation functional[34]—the B3LYP hybrid exchange correlation (XC) functional. We also used Wachters' all electron basis on iron, a 6-311++G^{2d} basis for all atoms directly bonded to iron, and a 6-31G* basis for the more distant atoms. A more detailed discussion of basis/functional/structural questions is given in the Results and Discussion section.

For the two heme model systems (CO)(pyr)(TPP)Fe and (PhNO)(pyr)(TPP)Fe and for the two DMG complexes, we used the following

(11) Strich, A.; Veillard, A. *Theor. Chim. Acta* **1981**, *60*, 379−383.
(12) Bytheway, I.; Hall, M. B. *Chem. Rev.* **1994**, *94*, 639−658.
(13) Malkin, V. G.; Malkina, O. L.; Casida, M. E.; Salahub, D. R. *J. Am. Chem. Soc.* **1994**, *116*, 5898−5908. Malkin, V. G.; Malkina, O. L.; Eriksson, L. A.; Salahub, D. R. In *Theoretical and Computational Chemistry*, Politzer, P., Seminario, J. M., Eds.; Elsevier: Amsterdam, 1995.
(14) Godbout, N.; Malkin, V. G.; Malkina, O. L.; Salahub, D. R. *J. Chem. Phys.* Submitted for publication.
(15) Eriksson, L. A.; Malkina, O. L.; Malkin, V. G.; Salahub, D. R. *Int. J. Quantum Chem.* **1997**, *63*, 575−583. Fedotov, M. A.; Malkina, O. L.; Malkin, V. G. *Chem. Phys. Lett.* **1996**, *258*, 330−335.
(16) Grodzicki, M.; Flint, H.; Winkler, H.; Walker, F. A.; Trautwein, A. X. *J. Phys. Chem. A* **1997**, *101*, 4202−4207.
(17) Godbout, N.; Havlin, R.; Salzmann, R.; Debrunner, P. G.; Oldfield, E. *J. Phys. Chem.* Submitted for publication.
(18) McMahon, M.; deDios, A. C.; Godbout, N.; Salzmann, R.; Laws, D. D.; Le, H.; Havlin, R. H.; Oldfield, E. *J. Am. Chem. Soc.* Submitted for publication.
(19) Breslow, R. *Org. Synth.* **1970**, *50*, 21. Breslow, R. *Org. Synth.* **1970**, *50*, 36.
(20) Piper, T. S.; Wilkinson, G. *J. Inorg. Nucl. Chem.* **1956**, *3*, 104−124.
(21) Sorriso, S.; Cardaci, G. *J. Organomet. Chem.* **1975**, *101*, 107−112.
(22) Piper, J. *J. Inorg. Nucl. Chem.* **1955**, *1*, 165.
(23) Harshani de Silva, D. G. A.; Lezhoff, D. B.; Impey, G.; Vernik, I. J. Z.; Stynes, D. V. *Inorg. Chem.* **1995**, *34*, 4, 4015−4025.
(24) Ping, S.-M.; Ibers, J. A. *J. Am. Chem. Soc.* **1976**, *98*, 8033−8036.
(25) Salzmann, R.; Wilson, S. R.; Havlin, R. H.; Oldfield, E. Unpublished results.
(26) Salzmann, R.; Ziegler, C.; Godbout, N.; McMahon, M.; Suslick, K. S.; Oldfield, E. *J. Am. Chem. Soc.* Submitted for publication.
(27) Gaussian 94, Revision E.2, Frisch, M. J.; Trucks, G. W.; Schlegel, H. B.; Gill, P. M. W.; Johnson, B. G.; Robb, M. A.; Cheeseman, J. R.; Keith, T.; Petersson, G. A.; Montgomery, J. A.; Raghavachari, K.; Al-Laham, M. A.; Zakrzewski, V. G.; Ortiz, J. V.; Foresman, J. B.; Cioslowski, J.; Stefanov, B. B.; Nanyakkara, A.; Challacombe, M.; Peng, C. Y.; Ayala, P. Y.; Chen, W.; Wong, M. W.; Andres, J. L.; Replogle, E. S.; Gomperts, R.; Martin, R. L.; Fox, D. J.; Binkley, J. S.; Defrees, D. J.; Baker, J.; Stewart, J. P.; Head-Gordon, M.; Gonzalez, C.; Pople, J. A.; Gaussian, Inc.: Pittsburgh, PA, 1995.
(28) Bühl, M. *Chem. Phys. Lett.* **1997**, *267*, 251−257.
(29) Wachters, A. J. H. *J. Chem. Phys.* **1970**, *52*, 1033−1036. Wachters, A. J. H. *IBM Technol. Rept. RJ584* **1969**.
(30) Basis sets were obtained from the Extensible Computational Chemistry Environment Basis Set Database, Version 1.0, as developed and distributed by the Molecular Science Computing Facility, Environmental and Molecular Sciences Laboratory, which is part of the Pacific Northwest Laboratory, P.O. Box 999, Richland, WA 99352, and is funded by the U.S. Department of Energy. The Pacific Northwest Laboratory is a multiprogram laboratory operated by Battelle Memorial Institute for the U.S. Department of Energy under contract DE-AC06-76RLO 1830. Contact David Feller, Karen Schuchardt, or Don Jones for further information.
(31) Hehre, W. J.; Ditchfield, R.; Pople, J. A. *J. Chem. Phys.* **1972**, *56*, 2257−2261.
(32) Becke, A. D. *Phys. Rev. A* **1988**, *38*, 3098−3100. Perdew, J. P. *Phys. Rev. B* **1986**, *33*, 8822−8824.
(33) Becke, A. D. *J. Chem. Phys.* **1993**, *98*, 5648−5652.
(34) Lee, C.; Yang, W.; Parr, R. G. *Phys. Rev. B* **1988**, *37*, 785−789.

procedures for energy convergence and electric field gradient (EFG) tensor calculations: Step 1, iron was represented by a LANL2DZ effective core potential[35] and 3-21G* basis sets were used for all other atoms, together with the B3LYP hybrid exchange−correlation functional.[27] Step 2, as in Step 1, but Wachters' all electron basis set[29,30] was used for iron. Step 3, as in Step 2, but a 6-31G* basis was used instead of the 3-21G* basis. Step 4, in the final calculations, we used the following locally dense basis: Wachters' all electron basis (62111111/3311111/3111) on iron, 6-311++G^{2d} for all directly attached atoms plus the oxygen in the CO group, 6-31G* for other atoms two bonds away from the iron, and 3-21G* bases elsewhere. For the calculation of (CO)(1-MeIm)(TPP)Fe, Step 1 was done at the Hartree−Fock level with Wachters' iron basis set and 3-21G* on all other atoms. In Step 2, the basis sets on the first shell of atoms were replaced by 6-31G*. In Step 3, as in Step 2, but with the B3LYP XC functional. Step 4 was the same as described for the other systems. A similar approach was also used for the bis(pyridine), bis(*N*-methylimidazole), and bis(trimethylphosphine) adducts described below. The (CO)(pyr)-$(DMGBBN)_2$Fe and (CO)(1-MeIm)(TPP)Fe systems, shown in Figure 1, parts A and B, respectively, are examples of very large systems in which the locally dense basis approach was employed.

We also investigated the effects of CO ligand tilt and bend (τ and β) on the computed quadrupole splittings. Here, we used first of all a published porphyrin core geometry,[36] but the porphyrin ring substituents (at C^{β}) were replaced by hydrogens, and an axial imidazole was included, oriented in the same way as reported in the crystal structure of carbonmonoxymyoglobin.[37] We carried out theoretical, quantum chemical geometry optimizations of the Fe−C and C−O bond lengths at fixed ligand tilt and bend angles using a B3LYP hybrid exchange-correlation functional, Wachters' (62111111/3311111/3111) Fe basis set, a 6-31G* basis on the carbonyl group and the five nitrogen atoms, together with a 3-21G basis on the remaining atoms. The definitions of tilt and bend we use are that tilt is the angle between the perpendicular to the porphyrin plane and the Fe−C bond vector (0° is untilted) and bend is the angle between the Fe−C and C−O bond vectors (0° is unbent). These Gaussian-94 geometry optimizations, and EFG calculations, were performed on a cluster of Silicon Graphics/Cray (Mountain View, CA) Origin-200 computers in this laboratory, in addition to use of SGI Origin-2000 and Power Challenge computers at the National Center for Supercomputing Applications (Urbana, IL), using up to eight processors. Finally, we also calculated the electric field gradients at iron in the three recently reported heme structures in carbonmonoxymyoglobin (recorded at pH values of 4, 5, and 6), using the experimentally deduced metalloporphyrin geometries.[38]

Results and Discussion

In Mössbauer spectroscopy, the observed spectra of low spin-d^6 iron complexes generally consist of a quadrupole split doublet having a peak separation, ΔE_Q, that is related to the elements of the electric field gradient tensor at the nucleus by:

$$\Delta E_Q = \frac{1}{2} e Q V_{zz} \left(1 + \frac{\eta^2}{3}\right)^{1/2} \qquad (1)$$

where e is the electron charge, Q the quadrupole moment of the $I^* = {}^3/_2$ 14.4 keV excited state, V_{zz} is the largest component of the EFG tensor, and by convention:

$$\eta = \frac{V_{xx} - V_{yy}}{V_{zz}} \qquad (2)$$

$$|V_{zz}| > |V_{yy}| > |V_{xx}| \qquad (3)$$

In the presence of an applied field, each molecule has its EFG oriented differently in the field, and consequently has a different Hamiltonian, with different eigenvalues. Numerical methods can, however, be used to evaluate such powder spectra as a function of V_{ii}, from which ΔE_Q, η, and the sign of ΔE_Q can be deduced.[39,40] We determined the zero-field ΔE_Q values for eleven of the compounds of interest, and typical results are shown in Figure 2, including results for the new system, (CO)-(TPP)(1-MeIm)Fe(II). We also determined both the sign and magnitude of ΔE_Q for three of these systems, as shown in Figure 3. The signs of ΔE_Q for the bis(pyridine), bis(1-methylimidazole) and bis(trimethylphosphine) metalloporphyrins were already deduced by Grodzicki et al.[16] and are shown in Table 1. For the remaining compounds, all values are taken to be positive, based on the excellent accord between experimental and theoretical signed and unsigned ΔE_Q values (see below), except in the case of (PhNO)(pyr)(TPP)Fe. Here, Mansuy et al. have determined a negative value for ΔE_Q in the related ^{i}PrNO adduct of TPP,[41] but with a similar ΔE_Q value to that we have determined. We then determined theoretically the ^{57}Fe electric field gradient tensor elements for the compounds discussed above, using the locally dense basis set approach together with the B3LYP hybrid exchange-correlation functional. These results are presented in Table 1.

Now, unfortunately, there has been considerable uncertainty over the years as to the actual magnitude of Q, the quadrupole moment of the excited iron nucleus ^{57}Fe^m, with values ranging from -0.19×10^{-28} to $+0.44 \times 10^{-28}$ m^2 having been reported.[42] However, in two recent studies,[42,43] the topic of the actual value of Q has been reinvestigated in great detail, and the most recent values determined for Q are $0.16(\pm 5\%) \times 10^{-28}$ m^2 [43] and $0.11(2) \times 10^{-28}$ m^2.[42] In this work, we use the most precise recent determination, $Q = 0.16(\pm 5\%) \times 10^{-28}$ m^2, to convert our theoretical V_{ii} results into the Mössbauer quadrupole splitting, ΔE_Q.

We show in Table 1, and graphically in Figure 4 (○), the results of our ΔE_Q calculations for the 14 compounds investigated. We find very good agreement between theory and experiment for the six systems where the sign is known unambiguously, and similarly good accord for the other eight where the sign was inferred. The slope of the correlation line for all 14 points is 1.04 (versus 1 for the ideal correlation), the R^2 value is 0.975, and the root-mean-square error of the calculated points from experiment is 0.18 mm s^{-1}. These results are very promising, since they suggest that quantum chemical methods may now be used with some confidence to investigate Mössbauer quadrupole splittings in even larger systems, such as the dimethylglyoximato complexes, and of course in metalloporphyrins as well. For example, for the (CO)(pyr) complexes of DMG, we compute ΔE_Q values of 1.15 and 1.41 mm s^{-1}, which compare quite favorably with the experimental results of 1.31 and 1.51 mm s^{-1}, Table 1. Similarly, in the (CO)(pyr) porphyrin system, even though the EFG is much smaller, there is likewise good accord: a computed 0.37 mm s^{-1} versus the 0.57 mm s^{-1} determined experimentally, Figure 2. Moreover,

(35) Hay, P. J.; Wadt, W. R. *J. Chem. Phys.* **1985**, *82*, 284−298.
(36) Kim, K.; Ibers, J. A. *J. Am. Chem. Soc.* **1991**, *113*, 6077−6081.
(37) Abola, E. E.; Bernstein, F. C.; Bryant, S. H.; Koetzle, T. F.; Weng J. Protein Data Bank In *Crystallographic Databases−Information Content, Software Systems, Scientific Applications*; Data Commission of the International Union of Crystallography; File No. 1MBC.
(38) Yang, F.; Phillips, G. N., Jr. *J. Mol. Biol.* **1996**, *256*, 762−774.
(39) Zimmerman, R. *Nucl. Instrum. Methods* **1975**, *128*, 537−541.
(40) Münck, E.; Groves, J. L.; Tumolillo, T. A.; Debrunner, P. G. *Computer Phys. Commun.* **1973**, *5*, 225−238.
(41) Mansuy, D.; Battioni, P.; Chottard, J.-C.; Riche, C.; Chiaroni, A. *J. Am. Chem. Soc.* **1983**, *105*, 455−463.
(42) Su, Z.; Coppens, P. *Acta Crystallogr.* **1996**, *A52*, 748−756.
(43) Dufek, P.; Blaha, P.; Schwarz, K. *Phys. Rev. Lett.* **1995**, *75*, 3545−3548.

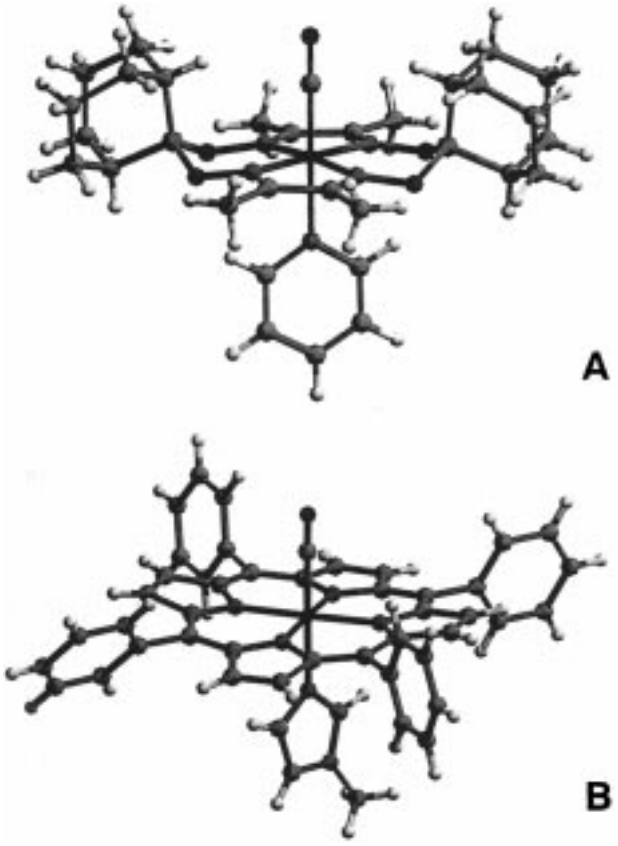

Figure 1. Structures of representative molecules used in calculations: (A) (CO)(pyr)(DMGBBN)$_2$Fe(II) and (B) (CO)(1-MeIm)(TPP)Fe(II).

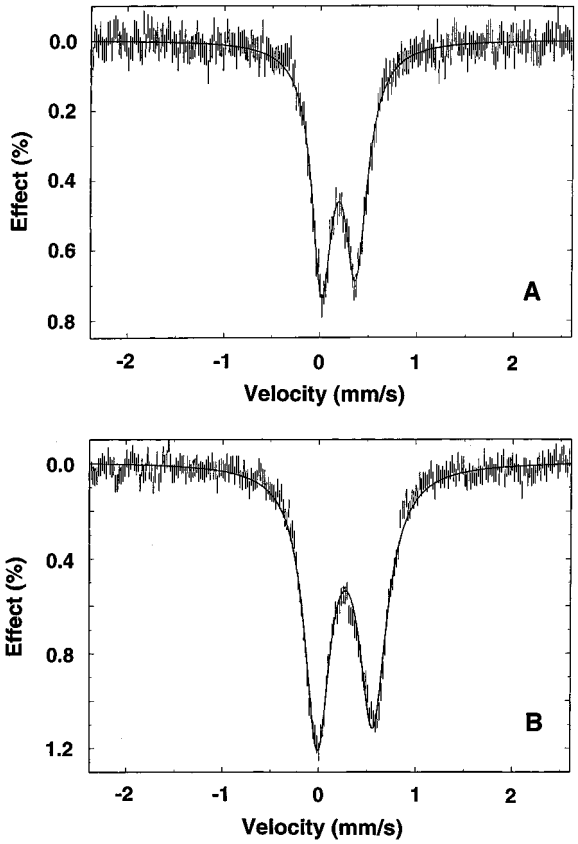

Figure 2. ^{57}Fe Mössbauer spectra of (A) (CO)(1-MeIm)(TPP)Fe(II) and (B) (CO)(pyr)(TPP)Fe(II) at $T = 77$ K and $B_0 = 0$ T.

the calculations also provide the correct sign for ΔE_Q, in each of the six systems where the sign has been determined experimentally. In addition, the root-mean-square errors between theory and experiment are quite small, and the slope between theory and experiment is very close to the ideal value of 1. At present, the origins of the residual errors which are seen are uncertain, and could originate from residual lattice effects, structural uncertainties, and motional averaging, as well as deficiencies in the basis sets and functionals used, and remaining uncertainties in the magnitude of the nuclear quadrupole moment itself. Of course, these are important questions, the answers to which will likely influence conclusions drawn from the calculations. We therefore chose to investigate further a wide variety of functional/basis set/structure/all electron-ECP combinations, to see to what extent the resultant EFGs (ΔE_Q) depended on these parameters. Results are given in Table 2. As anticipated based on Bühl's iron-57 NMR chemical shift work,[28] best accord with experiment is obtained when using the B3LYP hybrid functional, which incorporates Hartree−Fock exchange, rather than the pure BPW91 XC functional (calculations 1, 2 versus 3−10). More specifically, comparison between calculations 2 and 3 shows a major improvement with B3LYP. Use of effective core potentials (calculations 8−10) yields poor results for two different functionals and two decontraction schemes, as expected. There is also a small difference in ΔE_Q when using different Fe−C and C−O bond lengths, as shown in calculations 1 and 2, but the effect is minor. Removal of the phenyl rings causes only a small error (after correcting for the effects of the BPW91 functional, which clearly contributes $\sim$0.3 mm s^{-1}), calculations 2−4. Table 2 also shows the results of several locally dense basis calculations, which indicate no major effects are due to the mixed basis schemes used.

Also of interest in the results we have presented so far is the observation that the quadrupole splitting of the heme model compound, (CO)(NMeIm)(TPP)Fe, of 0.35 mm s^{-1}, Figure 2A, is extremely close to the $\sim$0.36−0.37 mm s^{-1} observed in carbonmonoxymyoglobin and carbonmonoxyhemoglobin.[7,44,45] Since this model compound has a linear and untilted Fe−C−O angle,[26] this similarity appears to support the notion of a linear and untilted Fe−C−O bond in the heme proteins themselves, but in order to test this hypothesis, it is necessary to investigate how the ^{57}Fe quadrupole splitting varies with ligand distortion. We therefore carried out a study of how ΔE_Q varies with ligand tilt and bend, using geometry optimization of the Fe−C and C−O bond lengths at each new geometry. Results for these optimized bond lengths, together with the total molecular eigenenergies, are given in Table 3. Clearly, the C−O bond length is quite constant over a wide range of geometries, although the Fe−C bond length varies rather more, Table 3. The results for the energies are generally consistent with those of Ghosh and Bocian[46] and Parinello et al.[47] For example, a 20° bend corresponds to a 3.1 kcal increase in energy in this study, to be compared with values of $\sim$3.5 and $\sim$3.1 kcal calculated by these workers.[46,47]

Next, we show in Table 4 and Figure 5 the results of the electric field gradient tensor calculations as a function of ligand tilt and bend, including both the quadrupole splitting, ΔE_Q, and the EFG asymmetry parameter, η, in Table 4. For carbonmonoxymyoglobin, the experimental value for the quadrupole

(44) Trautwein, A.; Maeda, Y.; Harris, F. E.; Formanek, H. *Theor. Chim. Acta (Berlin)* **1974**, *36*, 67−76.
(45) Parak, F.; Thomanek, U. F.; Bade, D.; Wintergerst, B. *Z. Naturforsch. Ser. C* **1977**, *32*, 507−512.
(46) Ghosh, A.; Bocian, D. F. *J. Phys. Chem.* **1996**, *100*, 6363−6367.
(47) Rovira, C.; Ballone, P.; Parrinello, M. *Chem. Phys. Lett.* **1997**, *271*, 247−250.

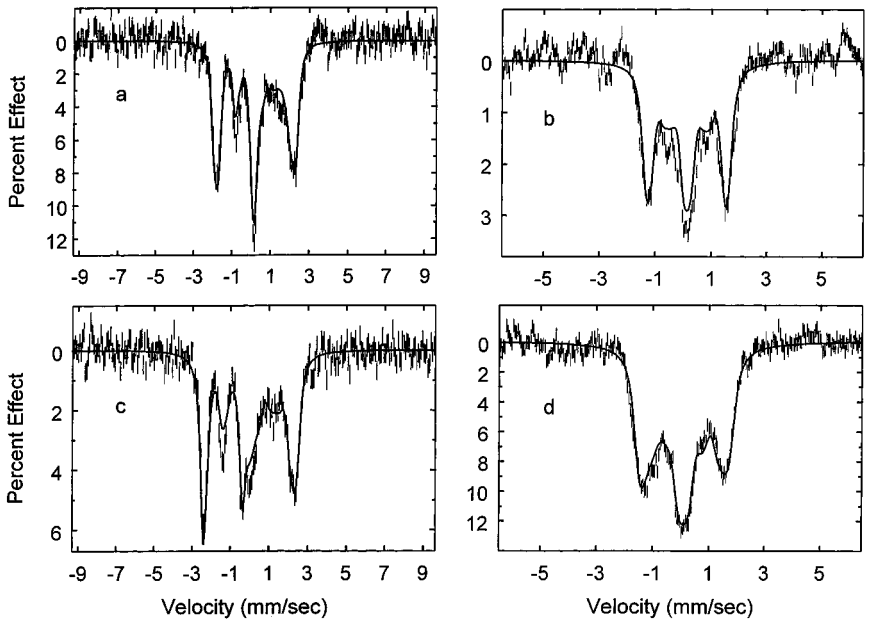

Figure 3. Zeeman perturbed ^{57}Fe Mössbauer spectra and simulations for four systems. (A) $CpFe(CO)_2Cl$: $T = 4.2$ K, $B_0 = 8.5$ T, $\Delta E_Q = +1.82$ mm s^{-1}, $\eta = 0.30$, $\delta = 0.27$ mm s^{-1}, Γ (width) $= 0.30$ mm s^{-1}. (B) $(CO)(pyr)(DMGBPh_2)_2Fe(II)$: $T = 4.2$ K, $B_0 = 6$ T, $\Delta E_Q = 1.23$ mm s^{-1}, $\eta = \sim 1.0$, $\delta = 0.15$ mm s^{-1}, $\Gamma = 0.32$ mm s^{-1}. The sign of ΔE_Q is indeterminate if η is exactly 1 but is assumed positive in Table 1 based on related DMG complexes having similar ΔE_Q, η values (ref 52). (C) $Fe(CO)_5$: $T = 4.2$ K, $B_0 = 8.5$ T, $\Delta E_Q = +2.52$ mm s^{-1}, $\eta = 0.4$, $\delta = 0$ mm s^{-1}, $\Gamma = 0.33$ mm s^{-1}. (D) (butadiene)$Fe(CO)_3$: $T = 4.2$ K, $B_0 = 6$ T, $\Delta E_Q = -1.34$ mm s^{-1}, $\eta = 0.4$, $\delta = 0.12$ mm s^{-1}, $\Gamma = 0.57$ mm s^{-1}.

Table 1. Eigenvalues of the Electric Field Gradient Tensor for ^{57}Fe in 14 Compounds Together with Calculated and Experimental Mössbauer Quadrupole Splittings

	electric field gradient tensor elements (au)			quadrupole splittings ΔE_Q (mm s^{-1})	
system	V_{11}	V_{22}	V_{33}	calcd	exptl
$Fe(CO)_3$(*cyclo*-butadiene)[a]	−0.988	0.477	0.510	1.60	1.52[b]
$Fe(CO)_5$[a]	−1.574	0.786	0.788	2.55	+2.51[c]
$Fe(CO)_3$(1,4-butadiene)[a]	−0.516	−0.384	0.903	−1.47	−1.34[c]
$CpFe(CO)_2Me$[a]	−1.190	0.216	0.974	2.05	1.76[b]
$Fe(CO)_3$(propenal)[a]	−1.149	0.073	1.076	2.08	1.70[b]
$CpFe(CO)_2Cl$	−1.167	0.443	0.724	1.91	+1.82[c]
$(CO)(pyr)(DMGBPh_2)_2Fe$	−0.616	0.010	0.606	1.15	1.31[b]
$(CO)(pyr)(DMGBBN)_2Fe$	−0.801	0.112	0.689	1.41	1.51[b]
(CO)(1-MeIm)(TPP)Fe	−0.269	0.110	0.159	0.44	0.35[b]
(CO)(pyr)(TPP)Fe	−0.223	0.063	0.161	0.37	0.57[b]
(PhNO)(pyr)(TPP)Fe	−0.561	−0.149	0.709	−1.21	−1.42[d]
$(pyr)_2$(TPP)Fe	−0.682	0.296	0.386	1.11	+1.15[e]
$(1\text{-MeIm})_2$(TMP)Fe	−0.613	0.220	0.393	1.00	+1.07[e]
$(PMe_3)_2$(OEP)Fe	−0.062	0.028	0.034	0.10	+0.35[e]

[a] Calculation performed at the geometry optimized structure. [b] ΔE_Q determined in this laboratory. [c] Signed ΔE_Q determined in this laboratory. [d] ΔE_Q determined in this laboratory; sign based on (iPrNO)(TPP)(nPrNH$_2$) (ref 41). [e] From ref 16.

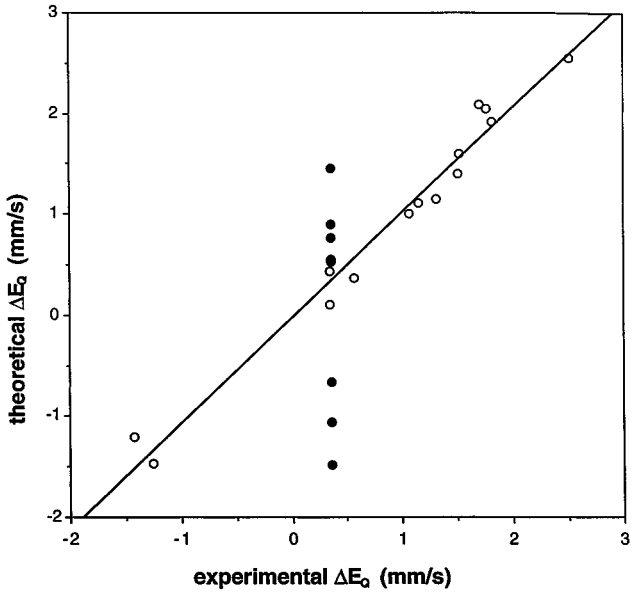

Figure 4. Graph showing the correlation between the experimental quadrupole splitting and that computed via DFT for the 14 compounds listed in Table 1 (○) and the tilt−bend results from Table 3 (●). The slope = 1.04, $R^2 = 0.975$, and the root-mean-square error = 0.18 mm s^{-1} for these 14 compounds. A Q value of 0.16×10^{-28} mm s^{-1} was used, as discussed in the text.

splitting is +0.363 to +0.373 mm s^{-1}, but the η value is more uncertain, with values of <0.4 to 0.75 mm s^{-1} having been reported.[44,45] For the geometry optimized structures we have investigated, Table 4, there is relatively close agreement for the quadrupole splitting and η between theory and experiment for the 0°,0° tilt−bend structure, where a value of 0.52 mm s^{-1} ($\eta = 0.283$) is obtained, Table 4 and Figure 5. However, the quadrupole splitting of the 20°, 20° geometry is also close to the experimental value, Table 4 and Figure 5, although its energy is some 11 kcal higher than the linear structure.

The effects of ligand tilt and bend on both the Mössbauer quadrupole splitting and the total molecular eigenenergy are shown graphically in Figure 6. Here, it can be seen that both ΔE_Q and the energy increase rapidly as the Fe−C−O group is bent, at a fixed 0° tilt. At a 20° tilt, ΔE_Q increases with increasing bend, and at ∼20° tilt, 20° bend, there is a very close agreement with the 0°, 0° ΔE_Q result as noted above, Figure 6. However, the energy penalty is very large, effectively ruling out such a conformation. Of course, these results alone cannot rule out small deviations from linearity, and other spectroscopic parameters, such as the ^{57}Fe NMR chemical shift, and the ^{13}C and ^{17}O NMR spectroscopic parameters will in the future all be needed in order to further refine the Fe−C−O structure, by using for example the Bayesian probability or Z-surface approach.[48] However, our results do support the idea of a very

Table 2. ^{57}Fe G94/DFT EFG Calculations for Model Iron CO *N*-Methylimidazole Porphyrins as a Function of Molecular Structure, Basis Sets, and Exchange-Correlation Functionals

system	structure[a]	functional	basis sets	q_{zz} (au)	q_{xx} (au)	q_{yy} (au)	ΔE_Q (mm/s)
1. Fe TPP	riding	B3LYP	Fe Wachters/6-311++G(2d) CO&N/6-31G* Cα/3-21G* others	−0.2686	0.1096	0.1591	0.44
2. Fe TPP	opt.	B3LYP	Fe Wachters/6-311++G(2d) CO&N/6-31G* Cα/3-21G* others	−0.3583	0.1522	0.2061	0.59
3. Fe TPP	opt.	BPW91	Fe Wachters/6-311++G(2d) CO&N/6-31G* Cα/3-21G* others	−0.5240	0.2317	0.2923	0.86
4. Fe P	riding	BPW91	Fe Wachters/6-311++G(2d) CO&N/6-31G* Cα/3-21G* others	−0.4322	0.1812	0.2510	0.71
5. Fe P	xray	BPW91	Fe Wachters/6-311++G(2d) CO&N/6-31G* Cα/3-21G* others	−0.4230	0.1841	0.2389	0.69
6. Fe P	C_2cap	BPW91	Fe Wachters/6-311++G(2d) CO/6-31G* others	−0.3088	0.1360	0.1728	0.50
7. Fe P	riding	BPW91	Fe Wachters/6-311++G(2d) CO&N/6-31G* porphyrin ring/3-21G* H	−0.4464	0.1876	0.2588	0.73
8. Fe P	riding	BPW91	Fe LANL2DZ/6-311++G(2d) CO&N/6-31G* Cα /3-21G* others	−0.6254	0.2888	0.3366	1.02
9. Fe P	riding	BPW91	Fe LANL2(Modif)/6-311++G(2d) CO&N/6-31G* Cα/3-21G* others	−0.7490	0.3515	0.3974	1.22
10. Fe P	riding	BPW91	Fe Stuttgart ECP/6-311++G(2d) CO&N/6-31G* Cα/3-21G* others	−0.6981	0.3262	0.3718	1.14
expt							0.35

[a] Riding = riding model geometry optimization, see ref 26 for details, d(C−O) = 1.094 Å; opt. = Fe−C, C−O geometry optimized (d(Fe−C) = 1.805 Å and d(C−O) = 1.149 Å), Table 3; X-ray = X-ray geometry, ref 26, d(C−O) = 1.061 Å; C_2-cap, the porphyrin structure is that of the C_2-cap CO iron porphyrin of Kim and Ibers (Kim, K.; Ibers, J. A. *J. Am. Chem. Soc.* **1991**, *113*, 6077−6081).

Table 3. Results of Geometry Optimization of the Fe−C and C−O Bond Lengths in the Fe−C−O Unit in (CO)(1-methylimidazole)(porphinato)iron(II) as a Function of Ligand Tilt and Bend[a]

angles (deg)		bond lengths (Å)		
tilt	bend	Fe−C	C−O	energy (hartrees)
0	0	1.8201	1.1476	−2586.34710992
0	20	1.8424	1.1475	−2586.34223258
0	40	1.9483	1.1454	−2586.32699571
20	0	1.7974	1.1512	−2586.32824784
20	20	1.8084	1.1524	−2586.33000569
20	40	1.8394	1.1477	−2586.31382686
40	0	1.8215	1.1641	−2586.24878457
40	20	1.8292	1.1565	−2586.23372963
40	40	1.8721	1.1521	−2586.15216391

[a] Structures were optimized by using G94/DFT with a B3LYP XC functional, Wachters' (62111111/3311111/3111) Fe basis set, 6-31G* on the CO group and the five attached nitrogen atoms, and 3-21G on the remaining atoms. The only parameters that were allowed to change during the geometry optimization were the Fe−C and C−O bond lengths.

Table 4. Eigenvalues of the Electric Field Gradient Tensor and Predicted Mössbauer Quadrupole Splittings and η Values for (CO)(1-methylimidazole)(porphinato)Fe(II) as a Function of Ligand Tilt and Bend[a]

ligand geometry		EFG tensor elements[b]				
tilt (deg)	bend (deg)	V_{11} (au)	V_{22} (au)	V_{33} (au)	η	ΔE_Q (mm s^{-1})
0	0	−0.3179	0.1140	0.2039	0.283	0.52
0	20	−0.4710	0.1645	0.3065	0.301	0.77
0	40	−0.8918	0.3561	0.5357	0.201	1.45
20	0	−0.3579	−0.0022	0.3601	0.99	−0.67
20	20	−0.3372	0.1296	0.2076	0.23	0.55
20	40	−0.5453	0.1720	0.3732	0.37	0.90
40	0	−0.5531	−0.3600	0.9131	0.21	−1.49
40	20	−0.4799	−0.1467	0.6266	0.53	−1.06

[a] The Fe−C and C−O geometries were from Table 3. [b] The locally dense basis/B3LYP approach was used to evaluate the Fe EFG, as described in the text.

close-to-linear and untilted Fe−C−O unit in carbonmonoxymyoglobin, not least because the splitting in the (CO)(NMeIm)(TPP)Fe system is virtually identical with that seen in MbCO.

In earlier work, a number of authors reported highly distorted Fe−CO units,[49−51] and very recently this idea has been

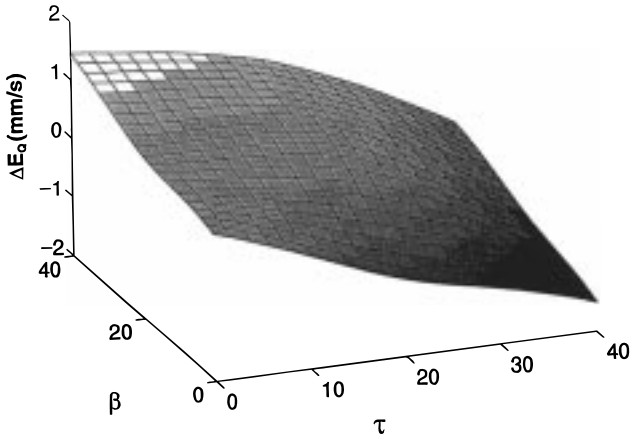

Figure 5. Iron-57 Mössbauer quadrupole splitting tilt−bend surface. ΔE_Q becomes more positive on increasing FeCO bend, but more negative with increasing tilt. τ and β are both in degrees.

reinforced for sperm whale $P2_1$ crystals at pH 4, 5, and 6, in which Fe−C−O bond angles of up to ∼125° have been reported.[38] Are these structures consistent with the Mössbauer results? To help answer this question, we have used the metallocycle geometries reported in the three recent crystallographic structures[38] to predict the corresponding ^{57}Fe Mössbauer quadrupole splittings. The results we have obtained are shown in Table 5, and the X-ray structures and their corresponding predicted quadrupole splittings are shown in Figure 7, together with results for the model (CO)(1-MeIm)(TPP)Fe compound. As can be seen from Table 5 and Figure 7, the predicted ^{57}Fe Mössbauer quadrupole splittings for the three distorted myoglobin structures are about 2 mm s^{-1}, five times larger than the experimental values of ∼0.36−0.37 mm s^{-1} for $P2_1$ sperm whale myoglobin, and the linear[26] (CO)(1-MeIm)(TPP)Fe model compound, where ΔE_Q = 0.35 mm s^{-1}, Figure 2A. In contrast, the calculated value for this model system is 0.44 mm s^{-1}, well within the 0.18 mm s^{-1} root-mean-square error found in Figure 4 for a range of compounds. These residual errors are most likely due to small structural uncertainties. For example, we find for the (CO)(1-MeIm)(TPP)Fe model a calculated ΔE_Q of 0.44 mm s^{-1}, but for the second linear/undistorted model structure based on the porphyrin of Kim and Ibers,[36] we calculate ΔE_Q = 0.52 mm s^{-1} (at the 0°, 0° tilt−bend geometry)—still within the 0.18 mm s^{-1} root-mean-square error noted above.

(48) Pearson, J. G.; Wang, J.-F.; Markley, J. L.; Le, H.; Oldfield, E. *J. Am. Chem. Soc.* **1995**, *117*, 8823−8829.

(49) Norvell, J. C.; Nunes, A. C.; Schoenborn, B. P. *Science* **1975**, *190*, 568−570.

(50) Powers, L.; Sessler, J. L.; Woolery, G. L.; Chance, B. *Biochemistry* **1984**, *23*, 5519−5523.

(51) Kuriyan, J.; Wilz, S.; Karplus, M.; Petsko, G. *J. Mol. Biol.* **1986**, *192*, 133−154.

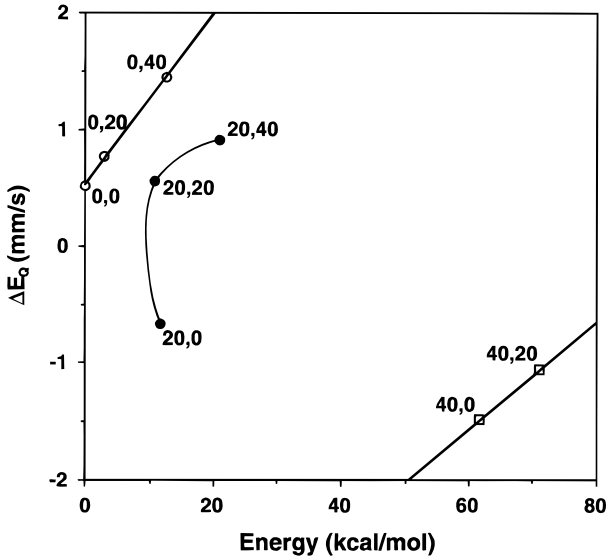

Figure 6. Graph showing the effects of Fe−C−O fragment tilt and bend geometry on the ^{57}Fe Mössbauer quadrupole splittings, and the change in total energy from that found in a linear, untilted system. The tilt and bend distortions are shown in degrees. The Fe−C and C−O bond lengths are given in Table 3.

Table 5. Eigenvalues of the Electric Field Gradient Tensor and Predicted Mössbauer Quadrupole Splittings and η Values for pH 4, 5, and 6 MbCO Model Systems and (CO)(1-methylimidazole)(5,10,15,20-tetraphenylporphinato)Fe(II)

system	EFG tensor elements[a] q_{zz} (au)	q_{xx} (au)	q_{yy} (au)	η	ΔE (mm s^{-1})
MbCO					
pH 4	−1.433	0.437	0.997	0.391	2.38
pH 5	−1.142	0.353	0.788	0.38	1.89
pH 6	−1.224	0.289	0.936	0.529	2.07
Fe(TPP)(CO)(1-MeIm)	−0.269	0.110	0.159	0.182	0.44

[a] Evaluated with the large locally dense basis set described in the text: Fe (62111111/3311111/3111)/6-311++G(2d)/6-31G*/3-21G*/B3LYP. The MbCO porphyrin structures were taken from ref 38.

Finally, it is worth noting that in addition to the eigenvalues of the electric field gradient tensor, the theoretical calculations also give the orientations of the EFG in the molecular frame, which in some cases can be compared with experimental results, and with predictions based on symmetry. For example, with the bis-amino complexes Fe(TPP)(pyr)$_2$ and Fe(TPP)(1-MeIm)$_2$, we find as expected[7] a close to axially symmetric tensor with V_{zz} oriented along the porphyrin normal, Figure 8A,B. With the Fe(TPP)(NMeIm)(CO) complex, our model for MbCO, V_{zz} is again oriented along the porphyrin normal Figure 8C, exactly as found in MbCO itself, at pH 7.[45] In calculations based on the pH 4, 5, and 6 crystallographic structures, V_{zz} is tilted from the heme normal (15° at pH 6, 18° at pH 5, and 24° at pH 4), with V_{zz} closely tracking the Fe−C bond vector, and single crystal Mössbauer studies of these systems would clearly be of interest.

Also of interest is the observation that linear and untilted Fe−C−O metallocycles do not necessarily have close to axially symmetric field gradient tensors. For example, in the case of the two dimethylglyoxime complexes, we find quite axially asymmetric tensors (η = 0.97, 0.72) with much larger ΔE_Q values than in MbCO or its model system. Large, positive ΔE_Q values (+1.19, +1.14 mm sec^{-1}) and relatively large η (0.55, 0.75) have been reported previously for other dimethylglyoximato CO adducts,[52] and it is clear that here, the asymmetry in the metallocycle−two separate dimethylglyoximato ligands,

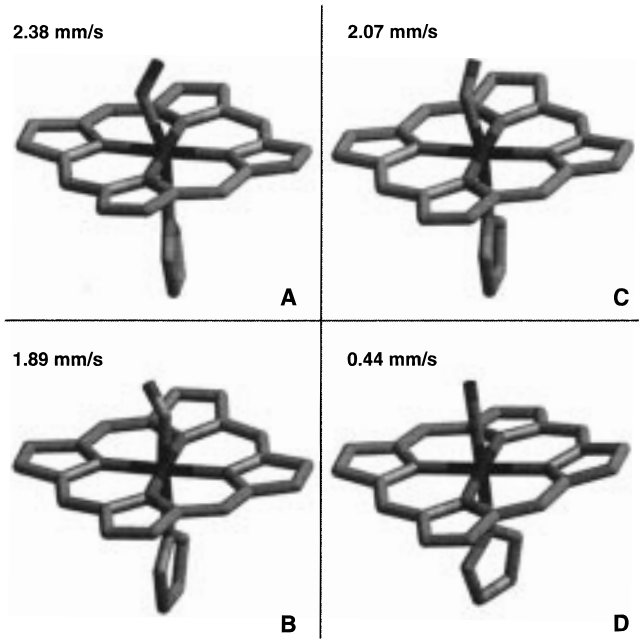

Figure 7. Figure illustrating the heme/Fe−C−O geometries found (ref 38) and Mössbauer quadrupole splittings predicted for *Physeter catodon* carbonmonoxymyoglobin, $P2_1$ crystallographic form, at different pH values, and in (CO)(1-MeIm)(TPP)Fe(II): (A) MbCO, pH = 4; (B) MbCO, pH = 5; (C) MbCO, pH = 6; (D) (CO)(1-MeIm)(TPP)Fe(II).

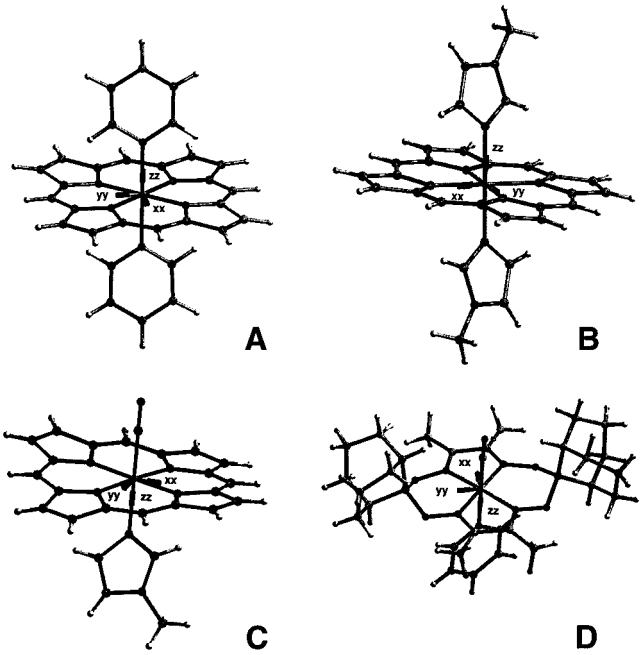

Figure 8. Orientation of the principal components of the ^{57}Fe electric field gradient tensors for four metallocycles: (A) (pyr)$_2$(TPP)Fe; (B) (1-MeIm)$_2$(TMP)Fe; (C) (CO)(1-MeIm)(TPP)Fe; and (D) (CO)(pyr)-(DMGBBN)$_2$Fe. The principal components, $|V_{zz}| \geq |V_{yy}| \geq |V_{xx}|$, are indicated.

contributes to the large η values found both experimentally and theoretically. However, V_{zz} is again oriented perpendicular to the plane of the metallocycle, as shown in Figure 8D.

In summary then, the results we have presented above indicate that iron-57 Mössbauer quadrupole splittings, at least for diamagnetic d^6 and d^8 systems, can now be predicted to an accuracy of ∼0.2 mm s^{-1}. For MbCO and HbCO, small (∼10°) ligand distortions cannot be ruled out based on either Mössbauer spectroscopic or purely energetic considerations alone, and

additional pieces of spectroscopic information, such as ^{13}C, ^{17}O, and ^{57}Fe NMR chemical shifts, will need to be considered for future refinements, as discussed elsewhere.[17,18]

Conclusions

The results we have presented above represent the first accurate calculations of ^{57}Fe Mössbauer quadrupole splittings in a wide variety of organometallic and metalloporphyrin complexes using density functional theory. The correlation between theory and experiment is good ($R^2 = 0.975$, root-mean-square error 0.18 mm s^{-1}) when all 14 compounds are considered, placing some confidence in the quality of the results obtained. The slope between theory and experiment is 1.05, using a Q value of 0.16×10^{-28} m^2. Of particular interest is the reproduction of the quadrupole splittings of macrocycles: dimethylglyoximato and porphinato complexes. This enables a test of the idea that Fe−CO geometries are highly distorted in the crystalline solid state in heme proteins, which they appear not to be. There is thus reason to be optimistic that ^{57}Fe Mössbauer quadrupole splittings, as well as electric field gradient tensor orientations, may now become even more useful in testing ideas about other metal−ligand geometries, such as with O_2, RNO, RNC, and R_2S ligands, and in paramagnetic systems as well, where related metal−ligand geometry questions exist.[53]

Acknowledgment. This work was supported in part by use of the SGI/Cray Origin 2000 and Power Challenge clusters at the National Center for Supercomputing Applications (funded in part by the US National Science Foundation, grant CHE-97002ON). We also thank Drs. Michael Bühl and Stephanie Vierkötter and Mr. Michael McMahon for helpful comments and communication of unpublished results.

JA972619F

(52) Morpurgo, G. O.; Mosini, V. *J. Chem. Soc., Dalton Trans.* **1974**, 2233−2237.
(53) Sage, J. T. *Appl. Spectrosc.* **1997**, *51*, 568−573.